SSC-193

The Superconducting Super Collider

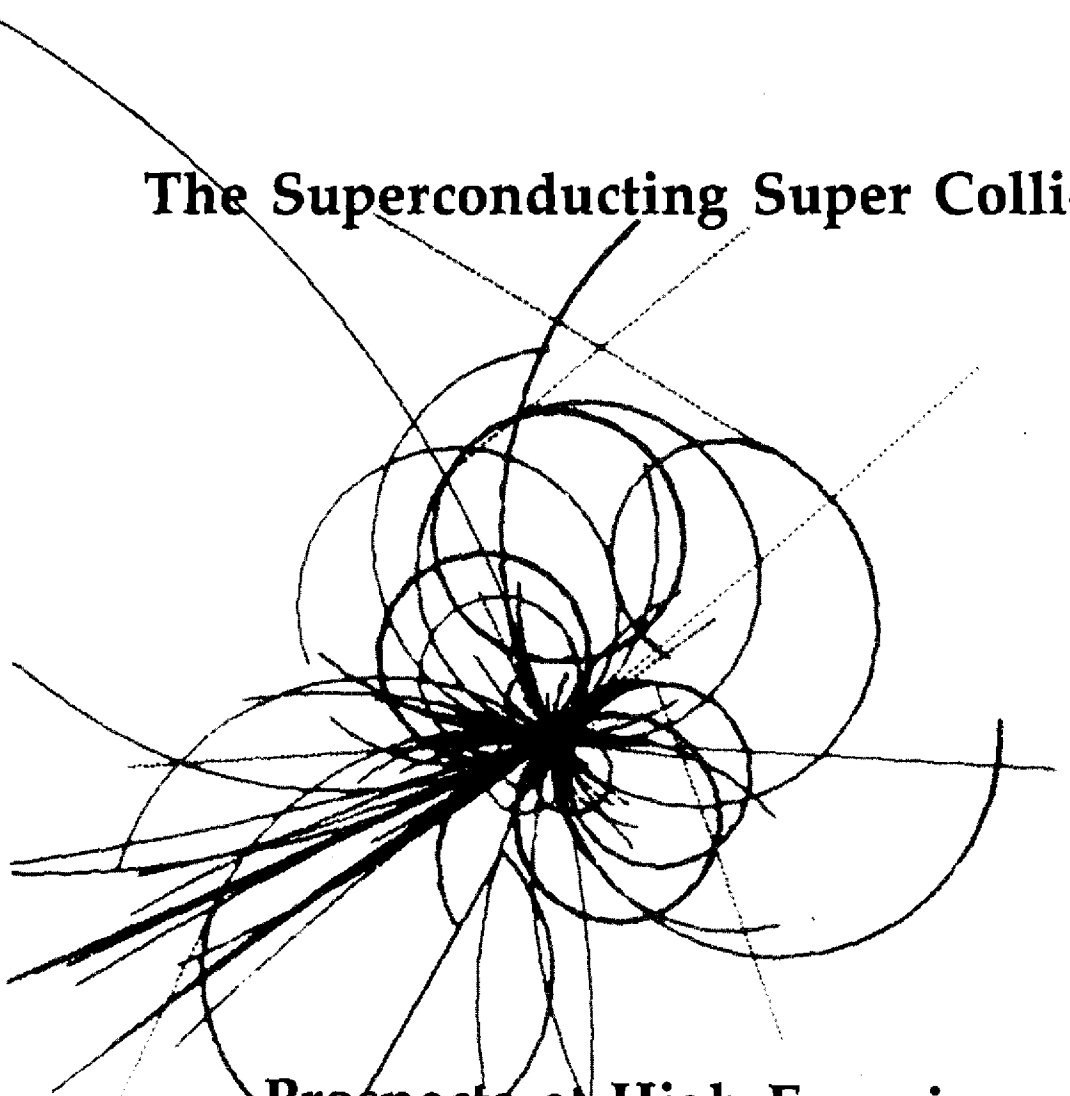

Prospects at High Energies

Chris Quigg

SSC Central Design Group

November, 1988

SSC-193

PROSPECTS AT HIGH ENERGIES*

Chris Quigg
SSC Central Design Group†
c/o Lawrence Berkeley Laboratory, Berkeley, California 94720

November 1988

*Presented at the 13th International Conference on Neutrino Physics and Astrophysics, Tufts University, Medford, Massachusetts, June 5–11, 1988.

†Operated by the Universities Research Association, Inc. for the Department of Energy.

PROSPECTS AT HIGH ENERGIES

CHRIS QUIGG
SSC CENTRAL DESIGN GROUP
LAWRENCE BERKELEY LABORATORY
BERKELEY, CA 94720 USA

1. ABSTRACT

I discuss some possibilities for neutrino experiments in the fixed-target environment of the SPS, Tevatron, and UNK, with their primary proton beams of 0.4, 0.9, and 3.0 TeV. The emphasis is on unfinished business: issues that have been recognized for some time, but not yet resolved. Then I turn to prospects for proton-proton colliders to explore the 1-TeV scale. I review the motivation for new physics in the neighborhood of 1 TeV and mention some discovery possibilities for high-energy, high-luminosity hadron colliders and the implications they would have for neutrino physics. I raise the possibility of the direct study of neutrino interactions in hadron colliders. I close with a report on the status of the SSC project.

2. FIXED-TARGET POSSIBILITIES

The prospects for fixed-target studies of neutrinos and their interactions are evolving as we move from the familiar ground of 400-GeV primary protons at Fermilab and CERN, through the 900-GeV regime opened by the Tevatron, toward the promise of 3-TeV protons at UNK. With this increase in energy has come a change in instrumentation marked by the demise of the large bubble chambers at CERN and Fermilab. What I shall present today is not new ideas—for I have none to offer—but established issues that we have not had the means to resolve. I will emphasize charged-current interactions of neutrinos, neglecting entirely the complementary studies now under way with the Tevatron muon beam and on the horizon for the electron-proton collider HERA. A definitive study of current

expectations for HERA experiments has just appeared.[1] The outlook for muon experiments at Fermilab is detailed in Kirk.[2] I refer to the rapporteur talk by Windmolders[3] at Munich for mention of the possibility of new muon experiments at CERN to reconcile the differences between EMC and BCDMS structure functions.

2.1 Structure Functions

The study of the structure of the nucleon in deeply inelastic scattering experiments is of continuing importance. The focus of attention has shifted over the years from the search for evidence in favor of the quark-parton model, to indications for deviations from Bjorken scaling anticipated in QCD and early measurements of the scale parameter Λ_{QCD}, to increasingly incisive tests of QCD. The evolution of the charged current cross section provides a basic test of our understanding of the strong interactions and may in the near future yield our first direct look at the effect of the intermediate boson propagator. Both these effects may be seen in the calculated total cross sections shown in Figure 1.

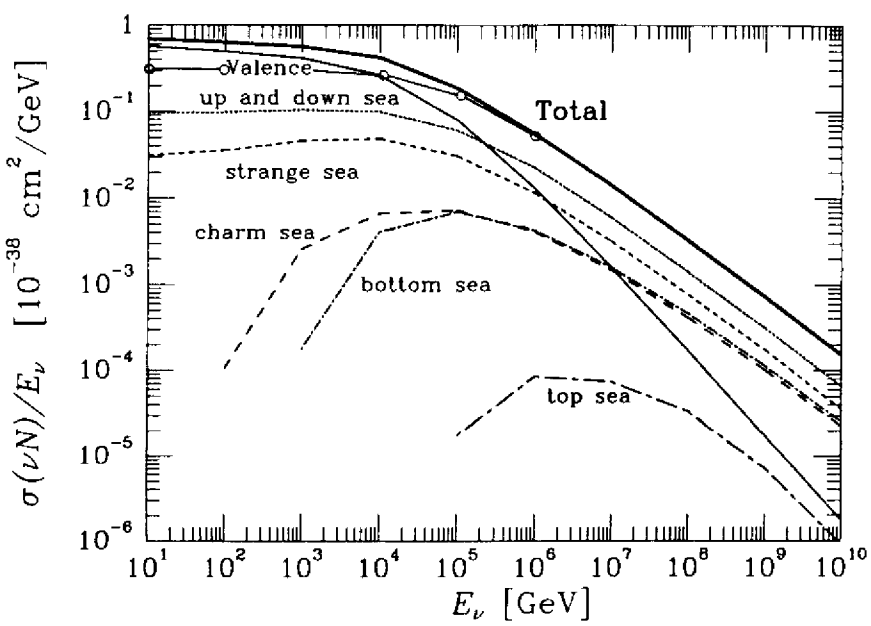

Figure 1: Total cross sections (divided by incident neutrino energy) for charged current interactions of neutrinos (thick solid line) and antineutrinos (circles) (from Ref. 4). Components of the νN cross section are displayed.

The slow decrease of the cross section for incident neutrino energies between 10^1 and 10^3 GeV is the familiar effect of the softening of the parton distribution with increasing Q^2 predicted in QCD. The more dramatic decrease of σ/E_ν at higher energies is a consequence of the W-propagator limiting the effective range in Q^2 to values not much larger than M_W^2. The same two effects are at work in the differential cross sections displayed for neutrino scattering in Figure 2(a). At low energies the distribution in the fractional energy loss y closely resembles the flat distribution of the valence quark approximation. In the absence of the intermediate boson propagator, the tendency in QCD is for both neutrino and antineutrino differential cross sections to approach the shape

$$\frac{d\sigma}{dy} \propto \frac{1}{2}\left(1+(1-y)^2\right) , \tag{2.1}$$

characteristic of a sea-dominated parton distribution. In terms of the mean value of y, the trend is from $\langle y_\nu \rangle = 1/2$ and $\langle y_{\bar{\nu}} \rangle = 1/4$ at low energies to $\langle y_\nu \rangle = \langle y_{\bar{\nu}} \rangle = 3/8$ at very high energies. This trend is evident in Figure 2(b), but it is superimposed on the propagator effect, which diminishes $\langle y \rangle$ further above about 10^4 GeV.

The predictions of QCD for the evolution of the quark-antiquark sea may also be tested in deeply inelastic neutrino scattering. The contributions of different flavors to the total cross section were indicated in Figure 1. The flavor content of the proton, as measured by the momentum fraction

$$\int_0^1 dx\, x\, f_i(x,Q^2) \tag{2.2}$$

carried by each parton species, is shown in Figure 3 for Set 2 of the EHLQ 1986 structure functions.[5]

As Q^2 increases, momentum is shared more and more equally among the quark and antiquark flavors, reflecting the trend toward the asymptotic values

$$\begin{aligned} \int_0^1 dx\, x\, G(x,Q^2\to\infty) &= \frac{8}{17} , \\ \int_0^1 dx\, x\, q_s(x,Q^2\to\infty) &= \frac{3}{68} \quad \text{(each flavor)}, \\ \int_0^1 dx\, x\, q_v(x,Q^2\to\infty) &= 0 , \end{aligned} \tag{2.3}$$

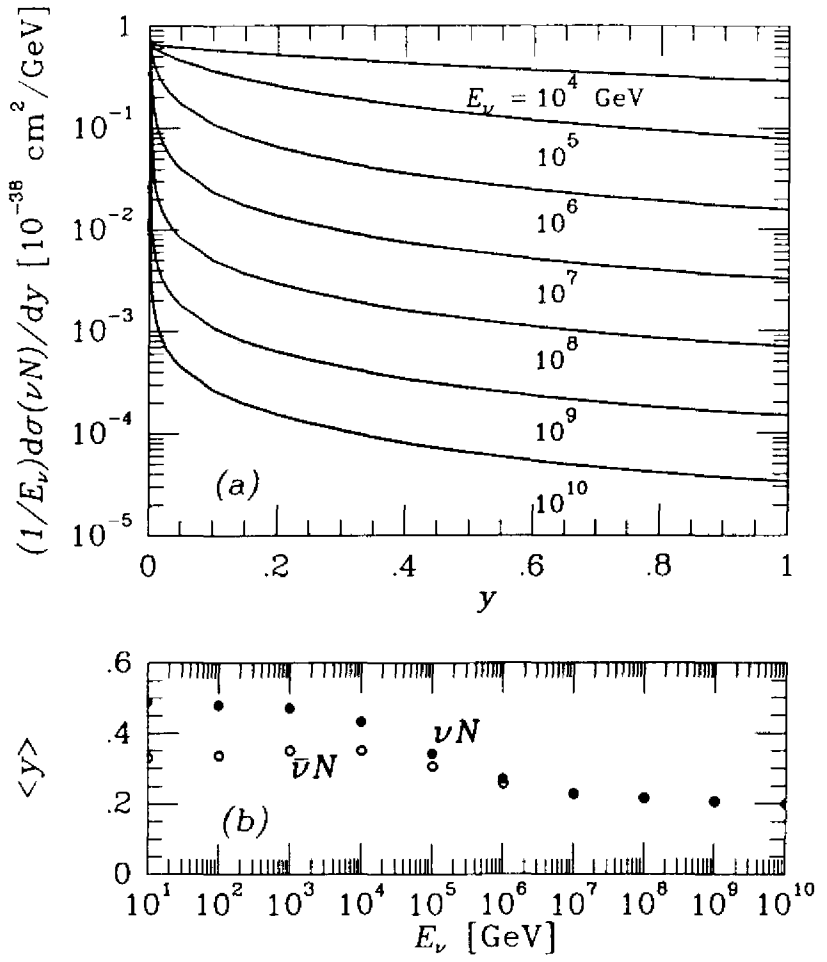

Figure 2(a): Differential cross sections for charged-current νN scattering; (b) mean values of the fractional energy loss parameter in νN and $\bar{\nu} N$ scattering (from Ref. 4).

expected in QCD with six quark flavors and no light colored superpartners. It is easy to verify that the momentum sum rule

$$\sum_{\text{i=parton species}} \int_0^1 dx\, x\, f_i(x,Q^2) = 1 \tag{2.4}$$

is satisfied:

$$\frac{8}{17} + 6 \text{ flavors} \times 2 \text{ (quarks + antiquarks)} \times \frac{3}{68} = 1. \tag{2.5}$$

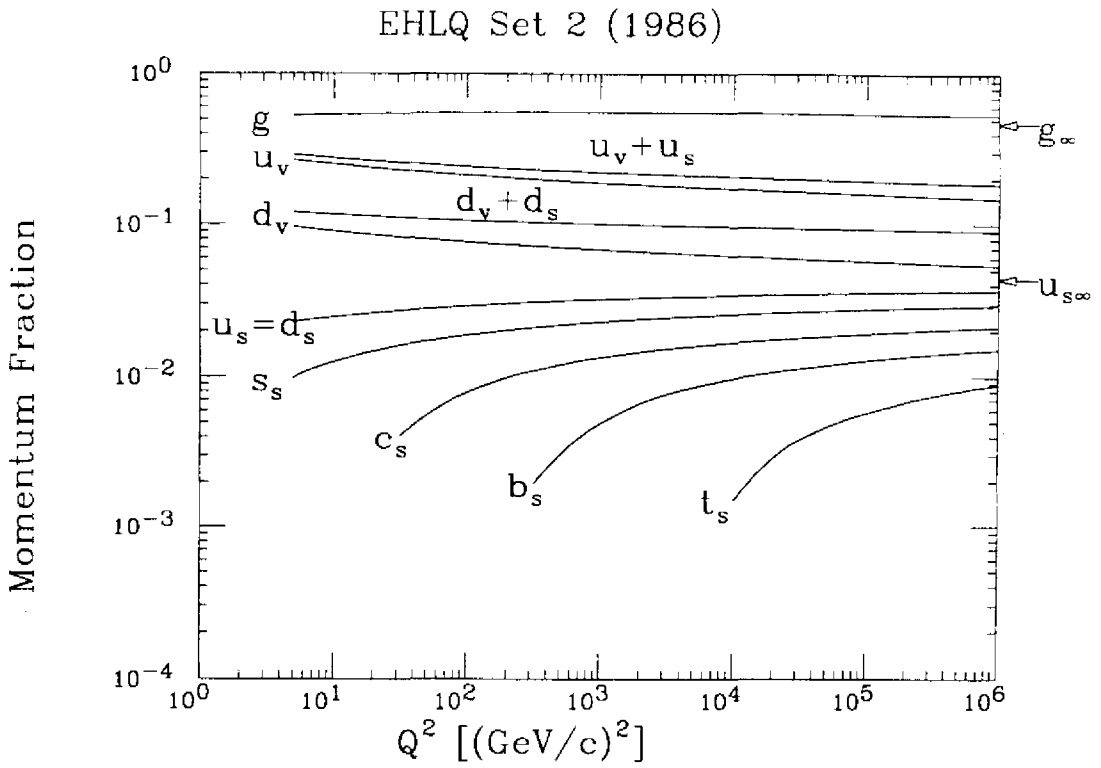

Figure 3: Momentum fractions of parton species in Set 2 of the 1986 EHLQ distributions.

The implications of QCD as $Q^2 \to \infty$ and $x \to 0$ are also of special interest to neutrino physics and are not so well known. The small-x behavior of the sea distribution is not constrained by experiments. Indeed, we cannot select among the asymptotic behaviors

$$x\, q_s(x,Q^2) \approx \left\{ \begin{array}{c} 0 \\ \text{finite} \\ 1/\sqrt{x} \end{array} \right\} \text{ as } x \to 0. \tag{2.6}$$

Fortunately, our ignorance of the small-x distributions for modest values of Q^2 is quickly washed away as $Q^2 \to \infty$, by the strong growth of the sea at small values of x, fed from the degraded valence distribution. It was noticed already in 1979 by Andreev, Berezinsky, and Smirnov[6] that the growth of the sea could have observable consequences for ultra-high-energy neutrino cross sections.

Since $Q^2 = 2ME_\nu xy$, the restriction on accessible values of Q^2 imposed by the W-propagator emphasizes the parton distributions in the region

$$x \approx M_W^2 / 2ME_\nu \ , \tag{2.7}$$

where the growth of the sea with increasing Q^2 enhances the cross section over the predictions of the parton model. Two recent developments have sharpened this observation and increased its relevance to experiments. First, spurred by interest in future hadron colliders, several groups have produced structure functions that make sense for small values of x and large values of Q^2. The EHLQ distributions,[5] for example, apply for $x > 10^{-4}$ and Q^2 up to 10^8 GeV^2. These permit reliable calculations of the consequences of QCD for neutrino–nucleon scattering, up to an incident neutrino energy of 10^{17} eV. Second, MacKay and Ralston[7] have remarked that the double logarithmic approximation to wee-x parton distributions[8] can be used to obtain an analytic form for the population of the quark-antiquark sea at small values of x and large values of Q^2. This analytic form may often be convenient; it is indispensable for extrapolating explicit structure functions toward $x = 0$ and therefore to their use at still higher neutrino energies. For 10^{19}-eV neutrinos, QCD enhances the cross section by a factor of 25 over the predictions of the parton model.[4] This effect is clearly important to making large-volume detectors practical.[9] It remains to be seen whether it is enough to permit early observation of ultra-high-energy neutrinos and study of astrophysical sources.

2.2 The Three-Neutrino Experiment

All of us take great pleasure in the award of the 1988 Nobel Prize in physics to our friends Leon Lederman, Mel Schwartz, and Jack Steinberger for their two-neutrino experiment.[10] The possibility of a "three-neutrino experiment" to establish that a neutral, penetrating beam of tau-neutrinos can interact with matter to produce tau leptons has been discussed at Fermilab since 1979.[11] We have good reason to believe that the tau neutrino exists, from the properties of tau decay, and is a distinct neutrino species. If ν_τ were identical with either $\bar{\nu}_e$ or $\bar{\nu}_\mu$ the partial decay rates $\Gamma(\tau \to e\nu\bar{\nu})$ and $\Gamma(\tau \to \mu\nu\bar{\nu})$ would differ by a factor of two. They are known to be equal, within experimental errors. Accelerator searches for the

transition $\nu_\mu N \to \tau$ + anything set limits on the Fermi coupling constant $G(\tau\nu_\tau = \nu_\mu)$ that are inconsistent with the τ-lifetime, which implies a coupling of universal strength. The assignment $\nu_\tau = \nu_e$ is at odds with our understanding of universality within the standard electroweak theory and is not supported by neutrino oscillation experiments.

The idea of the three-neutrino experiment follows at once from the celebrated two-neutrino experiment that distinguished ν_μ from ν_e. A proton beam is directed onto a beam dump from which there issues a beam of prompt neutrinos, including energetic tertiary ν_τs produced in the decay chain

$$\begin{array}{l} D_s \to \tau\nu_\tau \\ \quad\quad \hookrightarrow \nu_\tau + \ldots \end{array} \quad . \tag{2.8}$$

These neutrinos penetrate shielding and then interact in a target-detector to produce tau leptons by the charged-current reaction

$$\nu_\tau N \to \tau + \text{anything} \quad . \tag{2.9}$$

The taus themselves subsequently decay and may be identified and measured. The experiment is shown schematically in Figure 4.

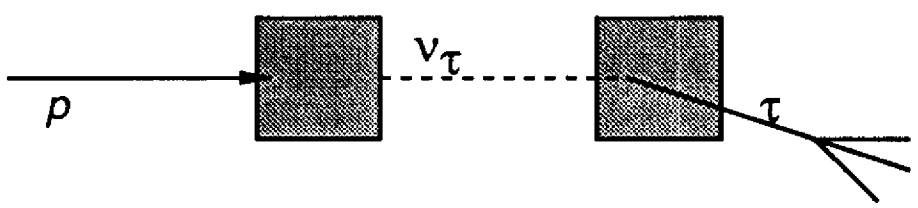

Figure 4: The three-neutrino experiment.

A beam dump and several experiments were designed, but never executed for these purposes, in part because many of the original goals, such as a measurement of the τ-lifetime, have been accomplished in other ways. It would still be satisfying to demonstrate the existence of the tau neutrino in this direct fashion.

What is new since the early discussions of the three-neutrino experiment? Until recently, the production of the charmed-strange meson D_s had not been observed in hadron collisions. The cross section for D_s production is of course a key ingredient in estimates of the event rate for a

three-neutrino experiment. The situation is still unsettled. However, a first observation has been reported[12] by Fermilab experiment E-400, in which neutrons with mean energy $< E_n > = 640$ GeV produce D_s (detected in the $\varphi\pi$ decay mode) in collisions with nuclear targets. The reported cross section $\times$ branching ratio is a surprisingly large value, $B\sigma \approx 1\ \mu b$. Further experimentation may well show that the harvest of ν_τs is not quite so bountiful as this first measurement would suggest. It is nevertheless encouraging that we are at last beginning to confront the question experimentally. A second new feature for three-neutrino experiments is the prospect of a 3-TeV primary proton beam at UNK. At this high energy, the taus will travel truly macroscopic distances before decaying. A crude estimate of the distribution of path lengths, scaled up from work done by Carl Albright and Shigeki Mori for Tevatron conditions, is shown in Figure 5.

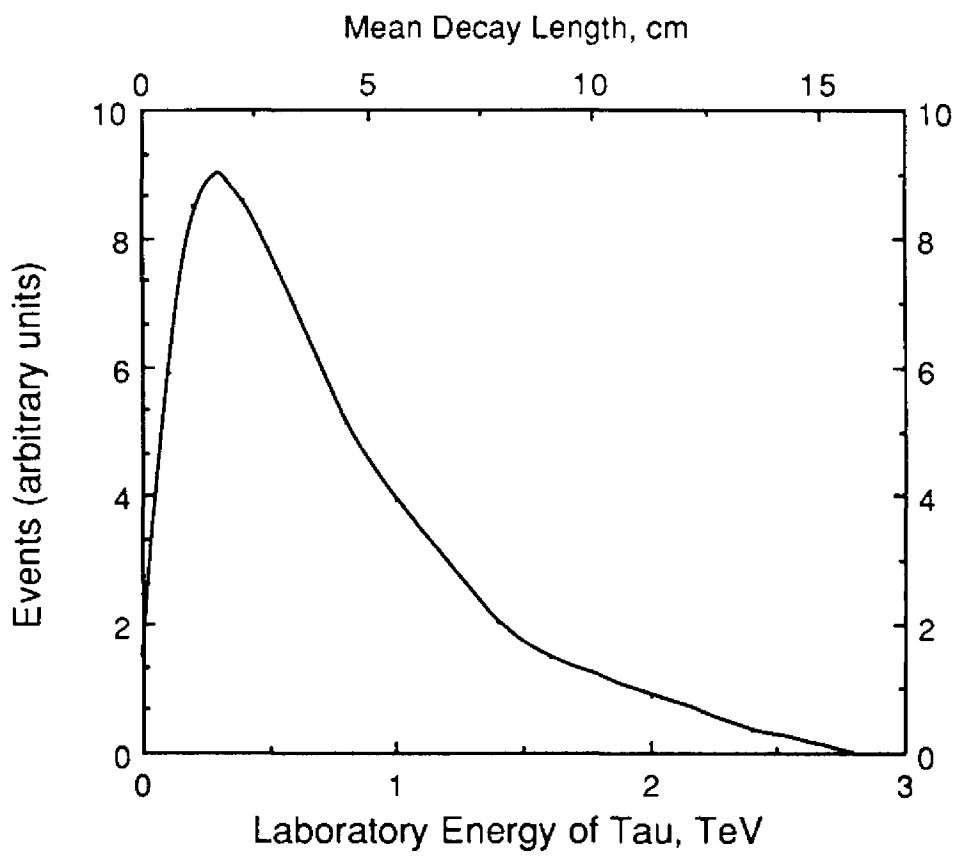

Figure 5: Laboratory energy distribution for tau leptons produced by tau-neutrinos created in a beam dump by 3-TeV protons. The mean decay length is indicated as a function of energy.

Many of the taus travel several centimeters before decaying. What does this suggest for the characteristics of a detector to carry out the three-neutrino experiment at UNK?

2.3 The Weak Mixing Parameter $\sin^2\theta_W$

In his talk at this conference, Marciano[13] has remarked that bounds on the proton lifetime, combined with the deviation from 0.21 of the weak mixing parameter $\sin^2\theta_W$ measured in neutral current interactions, imply that there must be more to life than a minimal unified theory based on the gauge group $SU(5)$. In other words, the desert hypothesis is inconsistent with these observations. While I am sympathetic with this conclusion, I am not convinced that the quoted errors on the weak mixing parameter accurately represent the unlikelihood that the "world average" value will change. The execution and analysis of neutral current experiments are highly nontrivial and demanding; I will not be surprised if, once again, $\sin^2\theta_W$ changes by appreciably more than an error bar.

3. WHY THERE MUST BE NEW PHYSICS ON THE 1-TEV SCALE

The Standard Model is incomplete;[14] it does not explain how the scale of electroweak symmetry breaking is maintained in the presence of quantum corrections. The problem of the scalar sector can be summarized neatly as follows.[15] The Higgs potential of the $SU(2)_L \otimes U(1)_Y$ electroweak theory is

$$V(\phi^\dagger\phi) = \mu_0^2\,(\phi^\dagger\phi) + |\lambda|(\phi^\dagger\phi)^2 \ . \tag{3.1}$$

With μ_0^2 chosen to be less than zero, the electroweak symmetry is spontaneously broken down to the $U(1)$ of electromagnetism, as the scalar field acquires a vacuum expectation value fixed by the low-energy phenomenology,

$$\begin{aligned} \langle\phi\rangle_0 &= \sqrt{-\mu_0^2/2|\lambda|} \\ &\equiv (G_F\sqrt{8})^{-1/2} \approx 175\ \mathrm{GeV}\ . \end{aligned} \tag{3.2}$$

Beyond the classical approximation, scalar mass parameters receive quantum corrections involving loops of particles of spins $J = 1$, $1/2$, and 0:

$m^2(p^2) = m_0^2 +$ 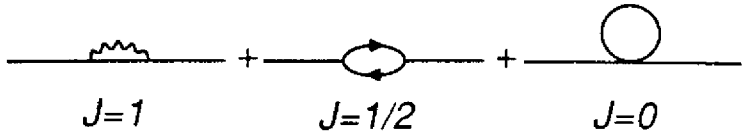

(3.3)

The loop integrals are potentially divergent. Symbolically, we may summarize the content of (3.3) as

$$m^2(p^2) = m^2(\Lambda^2) + Cg^2 \int_{p^2}^{\Lambda^2} dk^2 + \dots \ , \tag{3.4}$$

where Λ defines a reference scale at which the value of m^2 is known, g is the coupling constant of the theory, and C is a constant of proportionality, calculable in any particular theory. Instead of dealing with the relationship between observables and parameters of the Lagrangian, we choose to describe the variation of an observable with the momentum scale. In order for the mass shifts induced by radiative corrections to remain under control (i.e., not to greatly exceed the value measured on the laboratory scale), either (i) Λ must be small, so the range of integration is not enormous, or (ii) new physics must intervene to cut off the integral.

In the standard $SU(3)_c \otimes SU(2)_L \otimes U(1)_Y$ model, the natural reference scale is the Planck mass,

$$\Lambda \sim M_{\text{Planck}} \approx 10^{19} \text{ GeV} \ . \tag{3.5}$$

In a unified theory of the strong, weak, and electromagnetic interactions, the natural scale is the unification scale,

$$\Lambda \sim M_U \approx 10^{15} \text{ GeV} \ . \tag{3.6}$$

Both estimates are very large compared with the scale of electroweak symmetry breaking (3.2). We are therefore assured that new physics must intervene at an energy of approximately 1 TeV, in order that the shifts in m^2 not be much larger than (3.2).

Only a few distinct classes of scenarios for controlling the contribution of the integral in (3.4) can be envisaged. The supersymmetric solution[16] is especially elegant. Exploiting the fact that fermion loops contribute with an overall minus sign (because of Fermi statistics), supersymmetry balances the contributions of fermion and boson loops. In the limit of unbroken supersymmetry, in which the masses of bosons are degenerate with those of their fermion counterparts, the cancellation is exact:

$$\sum_{\substack{i = \text{fermions} \\ + \text{bosons}}} C_i \int dk^2 = 0. \tag{3.7}$$

If the supersymmetry is broken (as it must be in our world), the contribution of the integrals may still be acceptably small if the fermion-boson mass splittings ΔM are not too large. The condition that $g^2 \Delta M^2$ be "small enough" leads to the requirement that superpartner masses be less than about $1\ \mathrm{TeV}/c^2$.

A second solution to the problem of the enormous range of integration in (3.4) is offered by theories of dynamical symmetry breaking, such as technicolor.[17] In the technicolor scenario, the Higgs boson is composite, and new physics arises on the scale of its binding, $\Lambda_{TC} \approx 1$ TeV. Thus the effective range of integration is cut off, and mass shifts are under control.

A third possibility, which is appealingly economical but entails the sacrifice of perturbation theory for the electroweak interactions, is that of a strongly interacting gauge sector.[18] This would give rise to WW resonances, multiple production of Higgs bosons, and other new phenomena.

Nature may choose any (or none) of these human inventions, but we are driven unavoidably to the conclusion that some new physics must be found on the 1-TeV scale.

4. SOME HADRON COLLIDER DISCOVERY POSSIBILITIES

We have seen that the standard model hints that the frontier of our ignorance lies at about 1 TeV for collisions among the fundamental constituents. This conclusion is specific to the issue of electroweak symmetry breaking. More generally, the success of our theoretical framework suggests that a significant step is needed to see breakdowns of the

standard model. Hadron colliders offer a broad range of discovery possibilities when we take a large step into unexplored territory. Let us consider a few examples.

4.1 New Gauge Bosons

There are many reasons to be open to the possibility of new gauge bosons:

- High energy parity restoration in an $SU(2)_L \otimes SU(2)_R \otimes U(1)_Y$ electroweak gauge theory;
- The occurrence of extra $U(1)$ gauge symmetries, implying additional Z^0s, for example in unification groups larger than $SU(5)$;
- The low-energy gauge groups emerging from superstring models.

In a specific theory, the calculation of $W^{\pm}$ and Z^0 production rates is easily modified to yield an estimate of the cross section for the production of new gauge bosons. For the 40-TeV energy projected for the SSC, we may anticipate sensitive searches for a new W boson with standard gauge couplings to the light quarks out to a mass of about 6 TeV/c^2.

The exceptional group E_6 has a long history as a candidate group for the unification of the strong, weak, and electromagnetic interactions. Historically, the motivation for considering E_6 derived mainly from the observation that E_6 is the group beyond $SO(10)$, which is in turn the group beyond $SU(5)$:

$$E_6 \supset SO(10) \supset SU(5) \,. \tag{4.1}$$

The current revival is owed to the possibility that E_6 may be the surviving symmetry of the $E_8 \otimes E_8'$ internal symmetry group of the heterotic string.[19] Like all applications of superstring ideas to phenomenology, the "derivation" of E_6 is very vague and tentative. Nevertheless, it provides us with a reason to look again at some possible consequences of an E_6 gauge symmetry.

The spectrum of quarks and leptons can be read off from the fundamental **27** representation of the group:

$$
\begin{array}{llllllll}
E_6\text{:}\ \mathbf{27} = & \underbrace{\qquad\qquad\mathbf{16}\qquad\qquad} & \oplus & \underbrace{\qquad\qquad\mathbf{10}\qquad\qquad} & \oplus & \underbrace{\mathbf{1}} & : SO(10) \\
SU(5)\text{:} & \mathbf{10} \oplus \mathbf{5^*} \oplus \mathbf{1} & & \mathbf{5} \oplus \mathbf{5^*} & & \mathbf{1} & \\
 & u \quad d^c \quad N_e^c & & h \quad h^c & & n & \\
 & d \quad e & & E^+ \quad E^- & & & \\
 & u^c \quad \nu_e & & N_E^c \quad \nu_E & & & \\
 & e^c & & & & & \\
\text{charge } Q^{(\eta)} & -\frac{2}{3} \quad \frac{1}{3} \quad -\frac{5}{3} & & \frac{4}{3} \quad \frac{1}{3} & & -\frac{5}{3} &
\end{array}
\tag{4.2}
$$

The $\mathbf{10} \oplus \mathbf{5^*}$ of $SU(5)$ constitute the standard generation. The remaining member of the $SO(10)$ **16** is a right-handed neutrino. Among the novel particles characteristic of E_6, the new charge $-\frac{1}{3}$ weak isoscalar quark is of especial interest.

With respect to interactions, we are interested in a spontaneous symmetry breaking scheme that will lead eventually to $SU(3)_c \otimes SU(2)_L \otimes U(1)_Y$. Thus we wish to break

$$E_6 \to \cdots \to SU(3)_c \otimes SU(2)_L \otimes U(1)_Y [\otimes \mathcal{G}], \tag{4.3}$$

where $\mathcal{G}$ denotes possible additional symmetries that survive to low energies. There are examples in superstring theories of symmetry breaking induced by an E_6 adjoint **78** of Higgs bosons. This leads naturally to one or more extra $U(1)$ factors at low energies, which in turn implies an extra gauge boson, Z', coupled to a new conserved current corresponding to the charge $Q^{(\eta)}$.

To identify the gauge bosons (which lie in the adjoint **78** representation), we decompose

$$E_6 \supset SU(3)_c \otimes SU(3)_L \otimes SU(3)_R \ , \tag{4.4}$$

where the subscripts L and R denote left and right. The adjoint representation contains

$$78 = (8, 1, 1) \oplus (1, 8, 1) \oplus (1, 1, 8) \oplus (3^*, 3, 3) \oplus (3, 3^*, 3^*) . \tag{4.5}$$

The color octets are of course the familiar gluons. Among the $SU(3)_L$ octets, the particles transforming under $SU(2)_L$ as triplets or singlet are the $W^{\pm}$, Z^0, and γ. The color triplets are leptoquark gauge bosons. Finally, among the $SU(3)_R$ octets, the particle transforming as a singlet under $SU(2)_R$ corresponds to the new neutral gauge boson, Z'.

An additional neutral gauge boson is of interest because it may have observable consequences in the near future. Already, interesting limits can be set on the mass of the Z' by considering the effect it would have on neutral current processes. Consider, for illustration, a heavy Z', unmixed with the standard model Z^0, and with a (suitably defined) gauge coupling equal to that of the normal Z^0. Neutrino-quark neutral current processes would then be mediated by the exchange of both Z^0 and Z'. The contribution of the Z'-exchange diagram modifies the chiral couplings $L_\nu L_q$ and $L_\nu R_q$, which become

$$\begin{aligned} \tilde{L}_\nu \tilde{L}_q &= \tau_{3L} - 2e_q x_W \boxed{+Q_\nu^{(\eta)} Q_q^{(\eta)} x_W \cdot \left(\frac{M_Z}{M_{Z'}}\right)^2} \\ \tilde{L}_\nu \tilde{R}_q &= \quad\;\; - 2e_q x_W \boxed{+Q_\nu^{(\eta)} Q_q^{(\eta)} x_W \cdot \left(\frac{M_Z}{M_{Z'}}\right)^2} \end{aligned} \tag{4.6}$$

where $x_W = \sin^2\theta_W$. The extra neutral gauge boson suggested by many superstring theories couples to a charge $Q^{(\eta)}$, as listed in (4.2). The quantities $Q_\nu^{(\eta)}$ and $Q_q^{(\eta)}$ are the charges of the neutrino and quark under the new $U(1)$ symmetry. From the agreement of the measured u and d chiral couplings with the standard model, one may conclude[20] that

$$M_{Z'} \gtrsim 150\,\mathrm{GeV}/c^2. \tag{4.7}$$

The Z' is somewhat harder to produce in $p^{\pm}p$ collisions than a standard Z^0 of the same mass, because the couplings to light quarks are inhibited. In terms of the quark-antiquark luminosities defined in Ref. 5, for example, we may express the cross sections as

$$\sigma\begin{pmatrix} Z \\ Z' \end{pmatrix} = \frac{G_F \pi M_Z^2}{3\sqrt{2}} \sum_q \begin{pmatrix} L_q^2 + R_q^2 \\ \left(Q_q^2 + Q_{q^c}^2\right) x_W \end{pmatrix} \frac{\tau}{M^2} \frac{d\mathcal{L}_{q\bar{q}}}{d\tau}$$

$$\simeq 0.07 \cdot \left[\begin{pmatrix} 0.57 \\ 0.20 \end{pmatrix} \frac{\tau}{M^2} \frac{d\mathcal{L}_{u\bar{u}}}{d\tau} + \begin{pmatrix} 0.74 \\ 0.13 \end{pmatrix} \frac{\tau}{M^2} \frac{d\mathcal{L}_{d\bar{d}}}{d\tau} \right], \tag{4.8}$$

where $M = M_Z$ or $M_{Z'}$ and $\tau = M^2/s$. The branching ratio for the decay into charged leptons, for example, is

$$\Gamma(Z' \to e^+ e^-) \approx 3\%/n_g, \tag{4.9}$$

where n_g is the number of generations, which is somewhat smaller (by about $1/n_g$) than that of the conventional Z^0. The production cross sections for the new Z' are shown in Figure 6. We expect to be sensitive to this new object in the lepton pair channel for masses as large as about 3–4 TeV/c^2 in the SSC environment.

4.2 Sources of Heavy Quarks

The sources of heavy quarks are strong-interaction production in the reactions $gg \to Q\bar{Q}$ and $q\bar{q} \to Q\bar{Q}$ and electroweak production through the decays of $W^\pm$ and Z^0. The latter have the advantage of known cross sections—which is to say cross sections that can be measured from the leptonic decays of the gauge bosons—and calculable branching ratios. However, they lead to very large rates only for the decays of real (not virtual) gauge bosons. This makes them an attractive option for the top-quark search at the S$\bar{p}$pS and at the Tevatron.

The cross sections for the strong interaction processes are known in QCD perturbation theory:[21] The process $gg \to Q\bar{Q}$ is generally dominant and the reaction $q\bar{q} \to Q\bar{Q}$ generally makes a negligible contribution.

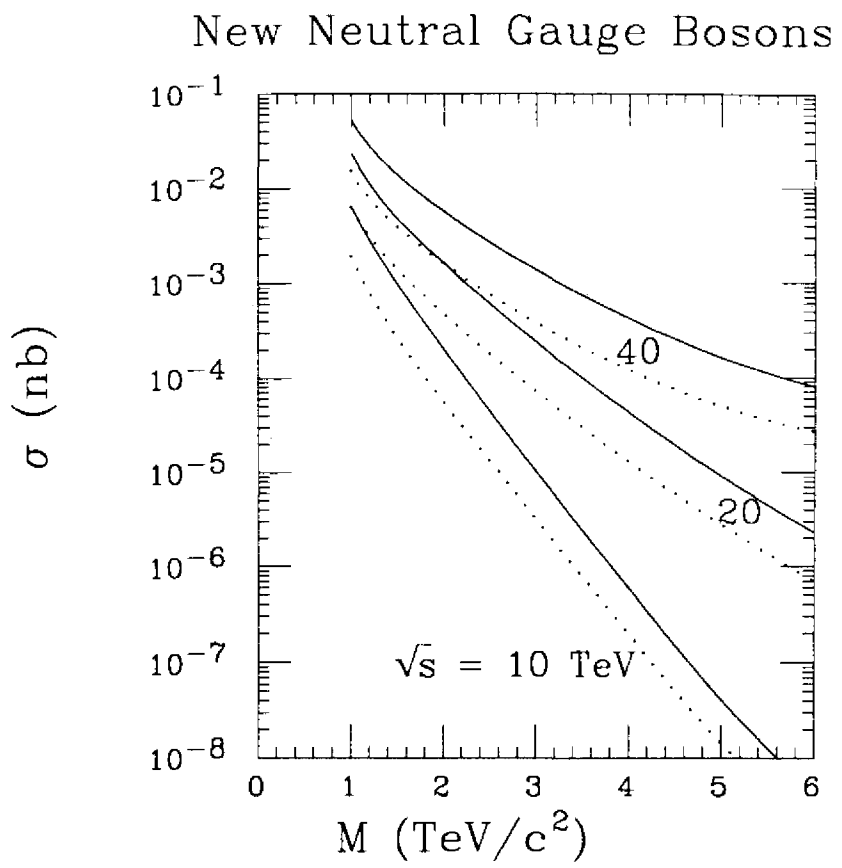

Figure 6: Cross section for the production of a heavy $Z^{0'}$-boson with rapidity $|y| < 1.5$ in pp collisions at 2, 10, 20, and 40 TeV. Solid lines: Weinberg-Salam couplings; dotted lines: E_6 couplings.

I show in Figure 7 the yield of heavy quarks from these sources for the $\bar{p}p$ colliders. Similar results are given for supercollider energies in EHLQ. A word of caution is in order for these estimates: when the "heavy quark" is light on the scale set by the elementary collisions, the next-order production process $gg \to gQ\bar{Q}$ may dominate.[22] A simple estimate will show why this is so. For $s_{Q\bar{Q}}/\hat{s} << 1$ and $\hat{s} >> 4M_Q^2$, we may approximate the cross section by considering the process

$$gg \to gg \quad \hookrightarrow Q\bar{Q} \quad , \tag{4.10}$$

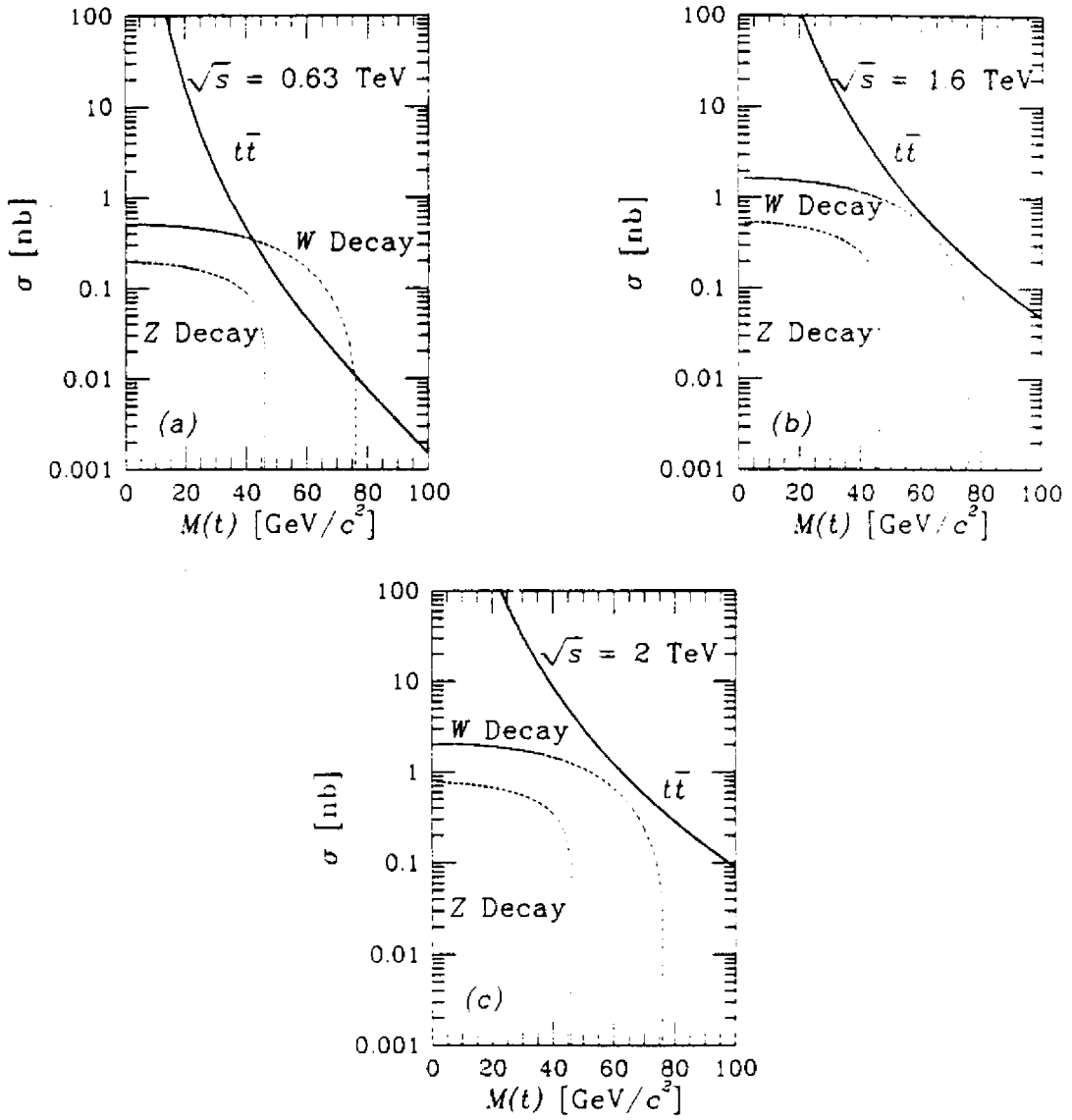

Figure 7: Cross sections for the production of t quarks or antiquarks in $\bar{p}p$ collisions as a function of the mass of the heavy quark. (a) $\sqrt{s}$ = 630 GeV; (b) $\sqrt{s}$ = 1600 GeV; (c) $\sqrt{s}$ = 2000 GeV.

the branching of a produced gluon into a $Q\bar{Q}$ pair. The ratio of three-body and two-body cross sections will be

$$\frac{\sigma(gg \to gQ\bar{Q})}{\sigma(gg \to Q\bar{Q})} \simeq \underbrace{\frac{\sigma(gg \to gg)}{\sigma(gg \to Q\bar{Q})}}_{O(100)} \cdot \underbrace{\frac{\alpha_s}{3\pi}}_{0.02} \cdot \underbrace{\log\left(\frac{\hat{s}}{4\,M_Q^2}\right)}_{2\text{–}4}$$

$$\simeq O(5-10), \tag{4.11}$$

where we have taken the ratio of the two-body cross sections at 90°. The three-body reaction mechanism is undoubtedly already preeminent for b-quark production at the S$\bar{p}$pS. The two mechanisms may in some measure be distinguished topologically. The $Q\bar{Q}$ final state leads to heavy quarks on opposite sides of the beam axis, whereas the $gQ\bar{Q}$ final state places both heavy quarks on the same side of the beam axis. A full $O(\alpha_s^3)$ calculation of the elementary cross section has been given recently.[23]

At the SSC, we expect an event rate sufficient for the discovery of heavy quarks with masses up to about 2 TeV/c^2.

4.3 Two-Jet Events

In a hadronic collision, useful kinematic variables are $p_\perp$, the transverse momentum of either jet, and the jet rapidities

$$y_i = \frac{1}{2} \log \left(\frac{E+p_z}{E-p_z} \right), \tag{4.12}$$

where p_z is the component of jet momentum along the beam direction. The dominant characteristic of many of these reactions is an angular dependence

$$\frac{d\sigma}{d\cos\theta^*} \sim \frac{1}{(1-\cos\theta^*)^2}, \tag{4.13}$$

arising from the t-channel gluon exchange, analogous to the t-channel photon exchange that drives the Rutherford formula. In terms of the variable $\chi \equiv \cot^2(\theta^*/2)$, the angular distribution may be reexpressed as

$$\frac{d\sigma}{d\chi} \sim \text{constant}. \tag{4.14}$$

I show in Figure 8 the angular distribution of two-jet events in the dijet c.m. frame, for dijets with effective masses in the interval

$$150\ \text{GeV}/c^2 < \mathcal{M}(\text{jet-jet}) < 250\ \text{GeV}/c^2, \tag{4.15}$$

as observed by the UA1 Collaboration.[24] To first approximation, the distribution is flat in χ, as our simple analogy with Rutherford scattering would suggest. In more detail, it agrees very precisely with the prediction of the parton model, shown as the solid curve.

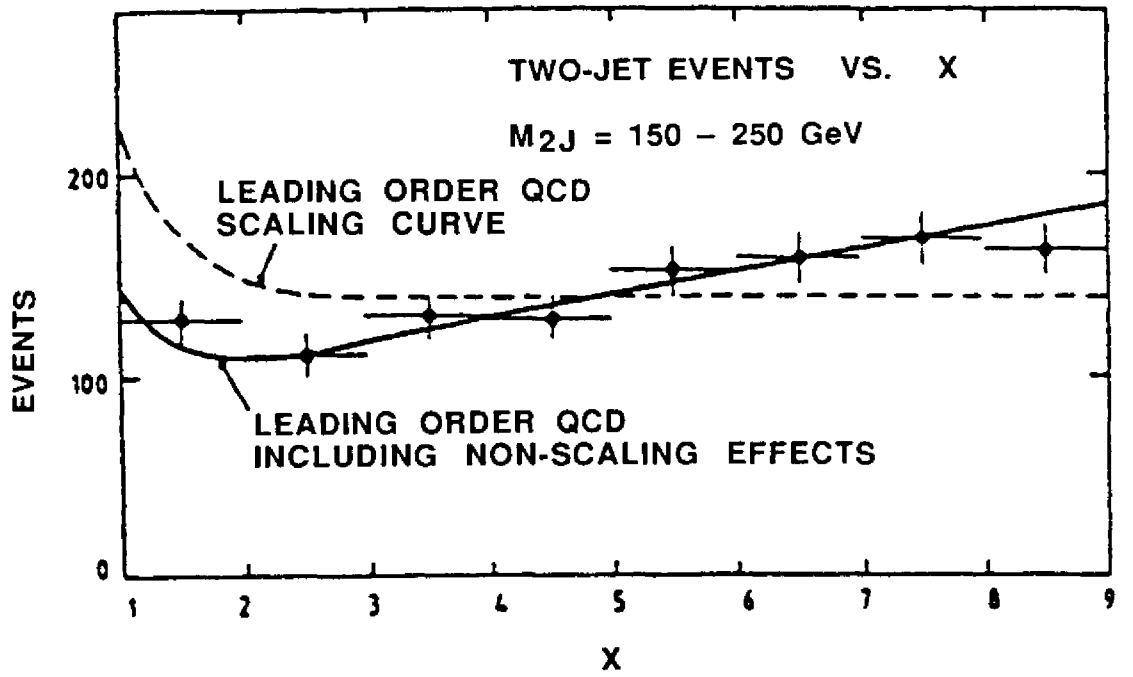

Figure 8: Angular distribution of two-jet events observed by the UA1 Collaboration in $\bar{p}p$ collisions at $\sqrt{s} = 540$ GeV, as described in the text. The curve shows the shape predicted by the QCD Born terms convoluted with the EHLQ structure functions (Set 1).

A further indication that the parton-model procedure is sound, and that knowledge of the structure functions derived from experiments on deeply inelastic lepton scattering is adequate, is provided by other S$\bar{p}$pS data on hadron jets. Figure 9 shows representative data from the UA1 Collaboration[25] on the inclusive jet cross section $d\sigma/dp_\perp dy\big|_{y\,=\,0}$, compared with the predictions of the QCD Born term. The agreement is quite satisfactory.[26]

Thus satisfied with the reasonableness of our procedure, we may make the extrapolation to supercollider energies. We first show in Figure 10 the one-jet differential cross section $d\sigma/dp_\perp dy\big|_{y=0}$ for pp collisions at 40 TeV. The figure shows separately the contributions of gluon-gluon final states ($gg \to gg$ or $q\bar{q} \to gg$, dot-dashed curves), gluon-quark final states ($gq \to gq$ or $g\bar{q} \to g\bar{q}$, dotted curves), and quark-quark final states ($qq \to qq$, $q\bar{q} \to q\bar{q}$, $\bar{q}\bar{q} \to \bar{q}\bar{q}$, or $gg \to q\bar{q}$, dashed curves).

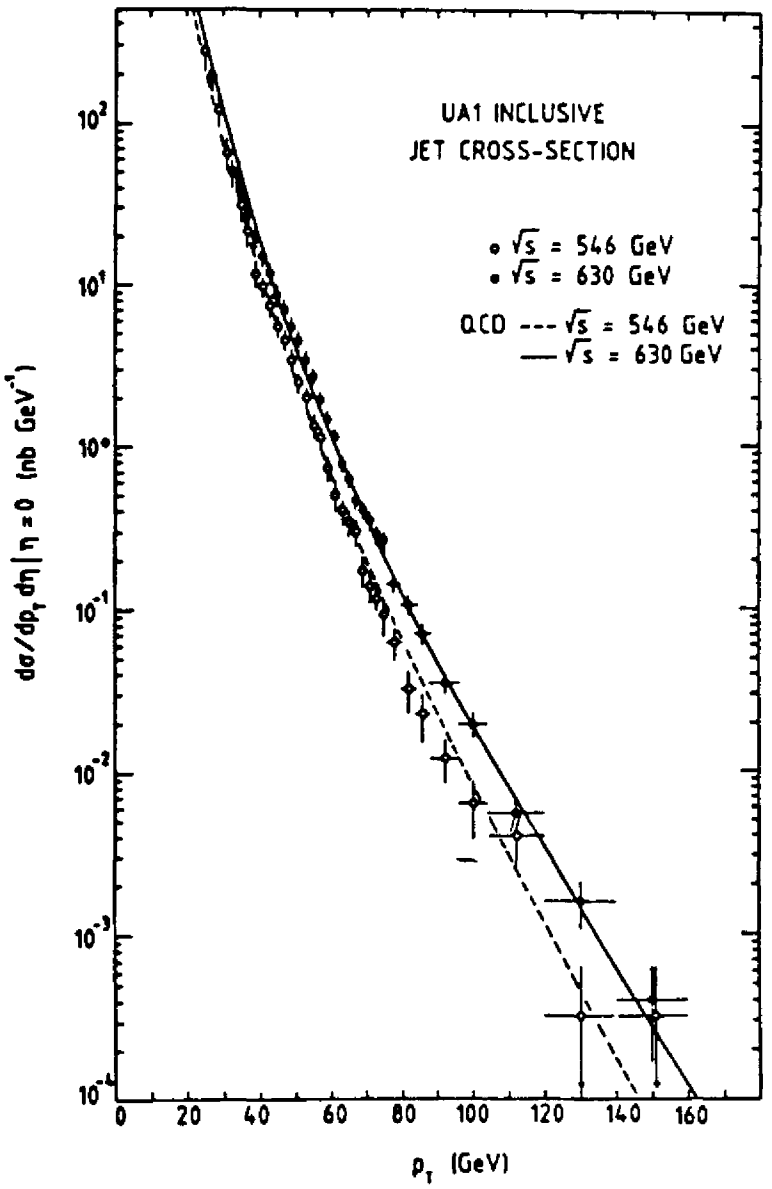

Figure 9: The inclusive jet cross section measured by the UA1 Collaboration for the pseudorapidity interval $|\eta| < 0.7$, as a function of the jet transverse momentum. The open dots correspond to the data at $\sqrt{s} = 546$ GeV and the solid dots to those at $\sqrt{s} = 630$ GeV.

Another interesting observable is the distribution of two-jet invariant masses $\mathcal{M}$. Figure 11 shows the mass spectrum $d\sigma/d\mathcal{M}$ for pairs of jets produced with $|y_i| < 1.5$ in 40-TeV pp collisions. Again the contributions of gluon-gluon, gluon-quark, and quark-quark final states are displayed separately. These jet-jet mass spectra represent a background for any new particles, such as new gauge bosons or Higgs bosons, that decay into jet pairs.

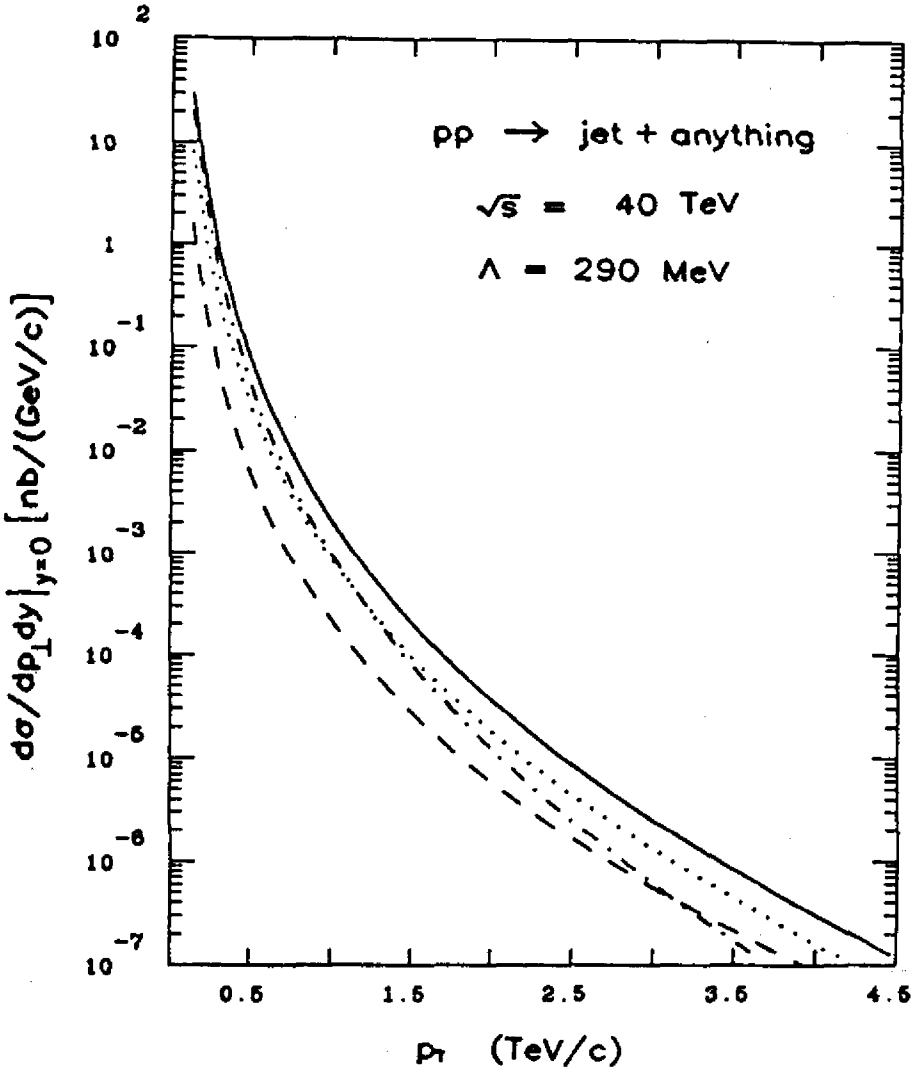

Figure 10: Differential cross section for jet production at $y = 0$ (90° c.m.) in pp collisions at 40 TeV, according to Set 2 of the EHLQ parton distributions. Dotted line: gg final state; dot-dashed line: gq final state; dashed line: qq final state; solid line: total.

4.4 Pairs of Gauge Bosons

Incisive tests of the structure of the electroweak interactions may be achieved in detailed measurements of the cross sections for the production of W^+W^-, $W^\pm Z^0$, Z^0Z^0, $W^\pm\gamma$, and $Z^0\gamma$ pairs. The rate for $W^\pm\gamma$ production is sensitive to the magnetic moment of the intermediate boson. In the standard model there are important cancellations in the amplitudes for W^+W^- and $W^\pm Z^0$ production that rely on the gauge structure of the WWZ

trilinear coupling. The Z^0Z^0 and $Z^0\gamma$ reactions do not probe trilinear gauge couplings in the standard model, but they are sensitive to nonstandard interactions such as might arise if the gauge bosons were composite. In addition, the W^+W^- and Z^0Z^0 final states may be significant backgrounds to the detection of heavy Higgs bosons and possible new degrees of freedom.

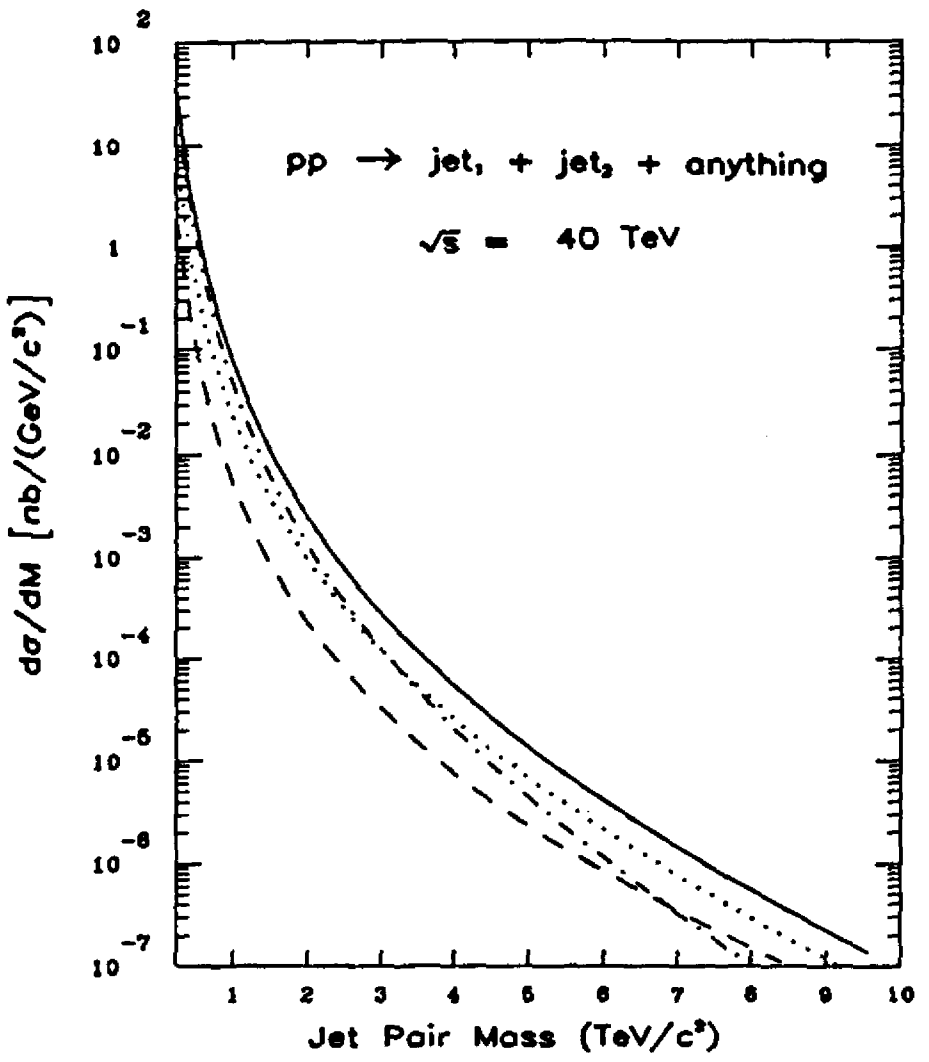

Figure 11: Invariant mass spectrum for two-jet events produced in proton-proton collisions at $\sqrt{s} = 40$ TeV, according to Set 2 of the EHLQ parton distributions. Both jets must satisfy $|y|<1.5$. Dotted line: gg final state; dot-dashed line: gq final state; dashed line: qq final state; solid line: total.

The intrinsic interest in the process $q_i\bar{q}_i \to W^+W^-$, which accounts in part for plans to study e^+e^- annihilations at c.m. energies around 180 GeV at LEP, is owed to the sensitivity of the cross section to the interplay among the γ-, Z^0-, and quark-exchange contributions. In the absence of the Z^0-exchange term, the cross section for production of a pair of longitudinally polarized intermediate bosons is proportional to E^2_{cm}, in gross violation of unitarity. It is important to verify that the amplitude is damped as expected. The mass spectrum of W^+W^- pairs is of interest both for the verification of gauge cancellations and for the assessment of backgrounds to heavy Higgs boson decays. This is shown for intermediate bosons satisfying $|y| < 2.5$ in Figure 12. The number of pairs produced at high energies seems adequate for a test of the gauge cancellations, provided that the intermediate bosons can be detected with high efficiency.

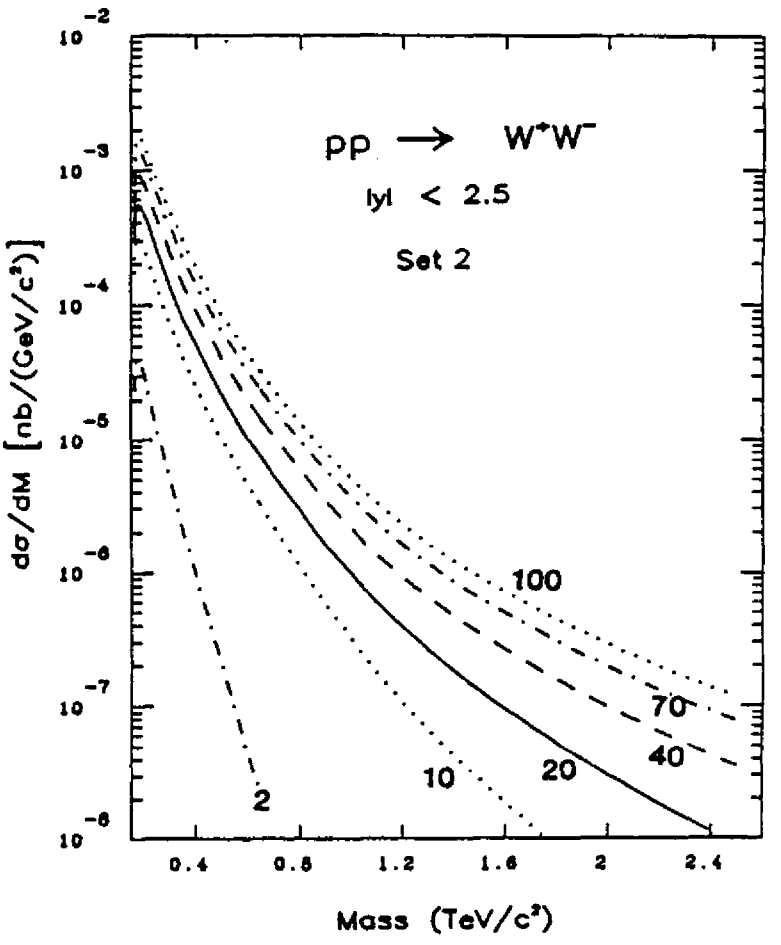

Figure 12: Mass spectrum of W^+W^- pairs produced in pp collisions at 40 TeV, according to the standard model and Set 2 of the EHLQ parton distributions. Both the W^+ and the W^- must satisfy $|y| < 2.5$.

Table 1 shows the expected yields of pairs of electroweak gauge bosons at the S$\bar{p}$pS, the Tevatron, and the SSC. At 630 GeV and an integrated luminosity of 10^{37} cm^{-2} = 10 pb^{-1}, prospects for the study of W^+W^- pairs are remote. It may be barely possible to initiate studies at 1.8 TeV and 10^{38} cm^{-2} = 100 pb^{-1}. At 40 TeV and 10^{40} cm^{-2} = 10^4 pb^{-1}, we can look forward to 2×10^6 W^+W^- pairs per year. Efficient detection is the key to incisive studies.

Table 1: Cross sections (in pb) for pair production of electroweak gauge bosons.

Pair	630 GeV $\bar{p}p$	1.8 TeV $\bar{p}p$	40 TeV pp
W^+W^-	0.43	6.4	214
$W^\pm Z$	0.51	1.65	73
ZZ	0.034	0.074	33

5. EXPERIMENTAL ENVIRONMENT OF THE SSC

What will experimentation be like at the SSC? Specific analysis of signals and backgrounds is quite fruitful and has been the object of many of the studies carried out over the past four years.[5, 27–32]

However, we must also be aware of the general environment in which detectors must function and events must be selected and recorded. The basic parameters of the SSC are set out in the Conceptual Design Report,[33] a non-site-specific conception of a 20 ⊕ 20 TeV proton-proton collider 83 km in circumference. The design calls for two clusters of interaction regions incorporating both physics experimental areas and major supporting equipment, a configuration that may be advantageous from the point of view of operating efficiency, economics, sociology, and accelerator physics. At the design luminosity of 10^{33} cm^{-2}sec^{-1}, interactions will occur at the rate of

$$0.016 \cdot (\sigma_t/1 \text{ mb}) \text{ interactions/crossing} \quad . \tag{5.1}$$

The length of each bunch of protons is 6.0–7.3 cm, and adjacent bunches are separated by 4.8 m.

We expect the total cross section at 40 TeV to lie in the range

$$100\,\text{mb} \lesssim \sigma_t \lesssim 200\,\text{mb}\ , \tag{5.2}$$

so that the event rate at the design luminosity may range up to 2×10^8 per second. The current best guess for the total cross section[34] is $\sigma_t = 138$ mb, of which about two-thirds is inelastic scattering.

A good way to gain respect for the conditions that will prevail at the SSC is to examine the trigger rate for events with transverse energy E_T greater than some threshold $E_T^{\min}$. This is shown in Figure 13 for the nominal operating conditions of the SSC: $\sqrt{s} = 40$ TeV and $\mathcal{L} = 10^{33}\text{cm}^{-2}\,\text{sec}^{-1}$, as well as at 10 and 100 TeV. At 40 TeV, a "high-E_T" trigger with threshold set at 2 TeV will count at 1 Hz from two-jet QCD events. This is of interest in planning triggers to efficiently select "interesting" events from the 2×10^8 interactions that will take place each second in an SSC interaction region.

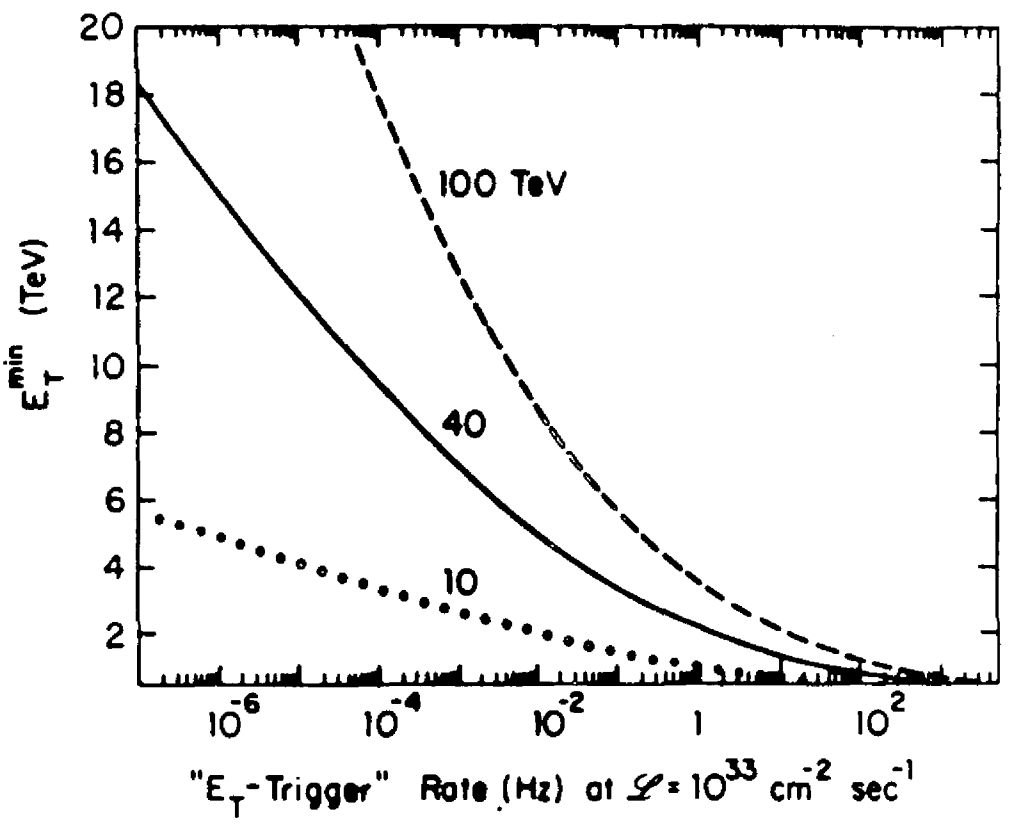

Figure 13: Counting rate for an E_T-trigger in pp collisions at an instantaneous luminosity of $\mathcal{L} = 10^{33}\text{cm}^{-2}\text{sec}^{-1}$. The threshold is defined for transverse energy deposited in the central region of rapidity, defined by $|y_i| < 2.5$ for jets 1 and 2.

Particle multiplicities will also be large. In QCD, we can estimate[35] the multiplicity of partons in a gluon jet as

$$\langle n(Q)\rangle_g \propto (\log Q/\Lambda)^{-c} \exp\left(\sqrt{\frac{12\log Q/\Lambda}{\pi b_0}}\right), \tag{5.3}$$

where $Q \approx p_\perp$ measures the virtualness of the jet, and

$$\begin{aligned} b_0 &= (33-2N_f)/12\pi \\ c &= (11+22N_f/27)/8\pi b_0 \end{aligned} , \tag{5.4}$$

where N_f is the number of active quark flavors. This result depends critically on taking account of quantum mechanical interference; in a purely probabilistic ("branching") approach, the exponent is larger by a factor of $\sqrt{2}$.

The multiplicity difference between quark jets and gluon jets is also calculable in perturbative QCD. The result[36] is

$$\frac{\langle n(Q)\rangle_g}{\langle n(Q)\rangle_q} = \frac{9}{4}\cdot(1 - 0.27\sqrt{\alpha_s} - 0.07\alpha_s) . \tag{5.5}$$

The multiplicity growth expected in quark jets, normalized to the observed multiplicity of hadrons produced in e^+e^- annihilations, is shown in Figure 14. There we see graphically the importance of including coherence effects. The multiplicities expected in a 1-TeV jet are impressively large.

Finally, the fragmentation of gluon jets into heavy quark pairs is expected to be reliably calculated in perturbation theory.[37] We expect about 0.1 $c\bar{c}$ pair per gluon jet at the S$\bar{p}$pS, and this is about what is seen.[38] For heavier flavors and higher energies, we may take some guidance from the evolution of a gg system into heavy flavors as given by perturbation theory, in Figure 15. Roughly speaking, a 1 TeV/c^2 gg system will yield 0.5 pair of c quarks, 0.25 pair of b quarks, and 0.05 t quarks.

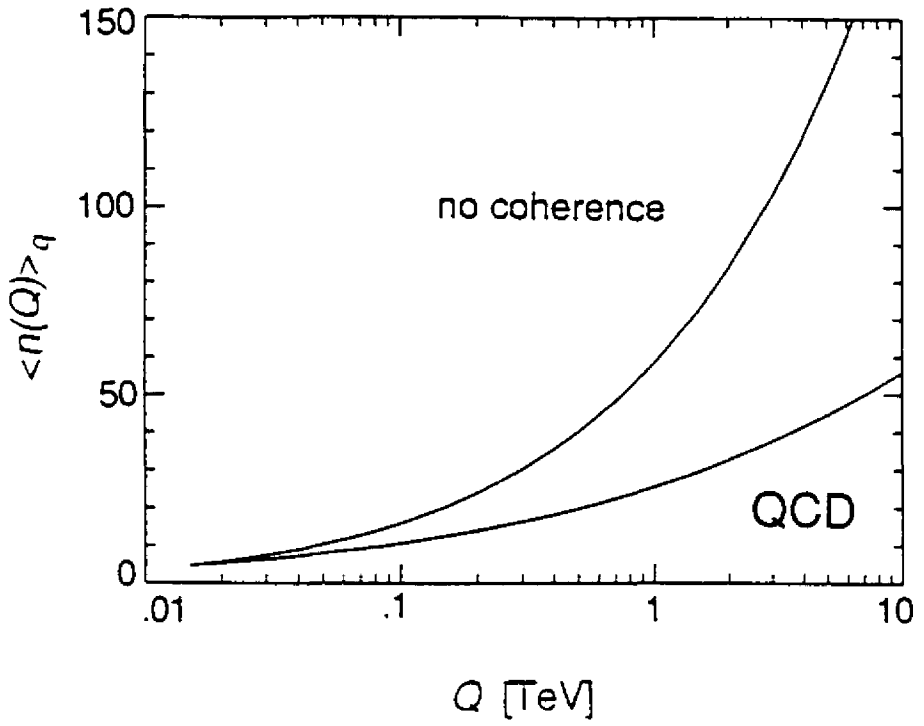

Figure 14: Growth of average multiplicity of hadrons produced in the fragmentation of a quark jet. For a jet produced at a hard interaction scale of 1 TeV, incoherent Monte Carlo programs overestimate the hadron multiplicity by more than a factor of 2. (From Ellis, Ref. 36.)

6. NEUTRINO PHYSICS WITH PROTON-PROTON COLLIDERS?

There are three principal obstacles to vigorous programs of neutrino physics with *pp* colliders. Most obvious is the need for extremely long decay spaces and muon filters, extending over tens of kilometers. Second, rapid-cycling fixed-target style operation places quite different demands on the magnets and accelerator systems from what is contemplated for collider operation. The SSC conceptual design calls for acceleration from 1 to 20 TeV over 1000 seconds. [The 60-second acceleration cycle planned for the high-energy (1-TeV) booster means that it will take about 30 minutes to load the two collider rings.] Finally, the LEP tunnel, a possible site for a hadron collider, is deep, and most of the sites considered for the SSC are deep as well. Excavation of the required decay spaces would be difficult and expensive.

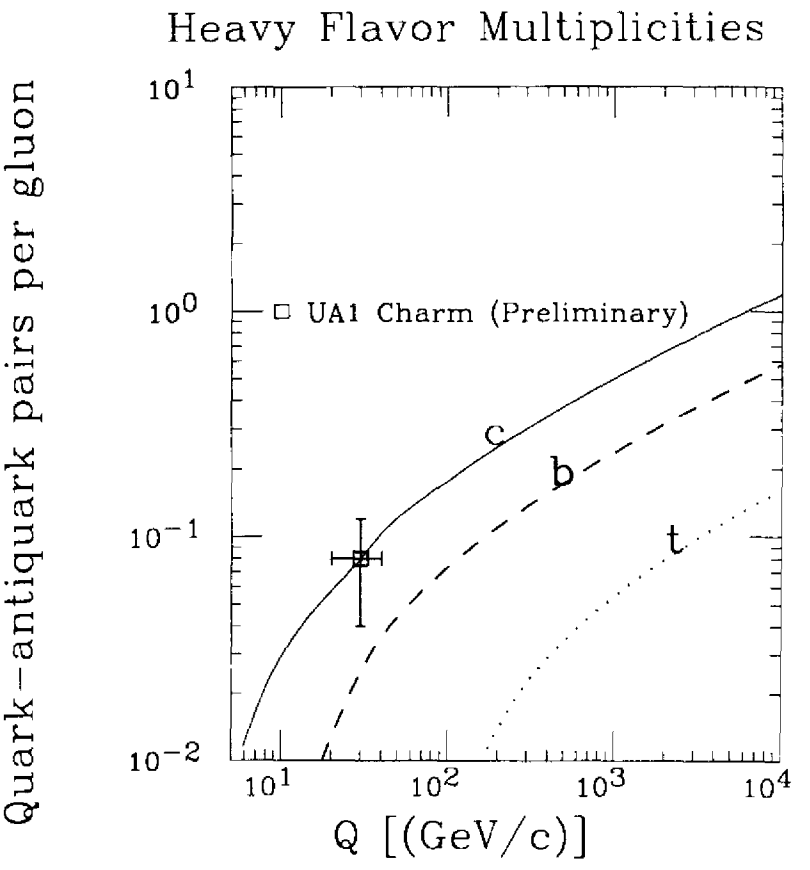

Figure 15: Evolution of gluon jets into heavy flavors, according to QCD perturbation theory (Ref. 37). For the curves shown, Λ = 200 MeV, and the masses of the charmed, bottom, and top quarks are 1.8, 5, and 40 GeV/c^2, respectively.

Whether because of these practical considerations or because of scientific judgments, there has been no great manifestation of community enthusiasm for fixed-target physics in general, or neutrino experiments in particular, at the SSC. There has, however, been some discussion of parasitic possibilities, but as yet too little honest toil to elaborate the practical details. One suggestion has been to use the 10^8 40-TeV collisions that occur each second in the interaction regions as prompt neutrino sources. Another has been to use slow extraction, lasting perhaps fifteen to thirty minutes, of the depleted beams to the beam dumps. This would provide approximately 10^{14} protons on target each day, to be exploited by neutrino detectors aimed at the dumps. For both of these cases, rates and backgrounds need to be worked out in detail, and the scientific motivation requires critical evaluation.

7. STATUS OF THE SSC PROJECT

The high-energy physics community in the United States has embarked on the design and eventual construction of a high-energy, high-luminosity, superconducting proton-proton collider to explore the 1-TeV scale. The SSC will produce collisions of 20-TeV proton beams at a luminosity of up to $10^{33}\,\mathrm{cm}^{-2}\mathrm{sec}^{-1}$, yielding more than 10^8 interactions per second.

Superconducting magnets are chosen for two reasons. First, they make possible confining fields three times as strong as those available with conventional iron magnets. More important, the electrical power requirements for a superconducting machine are far smaller than for a conventional accelerator. A conventional version of the SSC would consume 4 GW of electrical power; the SSC's average consumption will be about forty times smaller.

Even with the more intense fields made possible by superconducting magnets, the SSC will be an instrument of impressive size. In the engineering units appropriate to the problem, the bending radius is related to beam momentum and confining field by

$$\rho = \left(\frac{10}{3}\,\mathrm{km}\right)\cdot\left(\frac{p}{\mathrm{TeV}/c}\right) \Big/ \left(\frac{B}{\mathrm{tesla}}\right). \tag{7.1}$$

For a 20-TeV/c beam in a confining field of 6.6 T, the SSC design field, the implied radius of curvature is $\rho \approx 10$ km. With allowance for the straight sections accommodating experimental areas, acceleration gear, etc., the circumference of the SSC will be about 84 km.

The proposed layout of the Supercollider is shown in Figure 16. Interaction halls cluster on the two gently curved sides of the collider ring. In this perspective the near cluster incorporates the injector complex, the radio-frequency accelerating system, beam absorbers, and two of the six interaction halls. The far cluster adds four more interaction halls, two of which are reserved for development after research begins. The schematic enlargement of an interaction hall shows a detector surrounding the point at which two beams collide; the cross section to the right shows the position of the two superconducting magnet rings in the tunnel. The two independent rings for the proton beams will sit one atop the other, 70 cm apart.

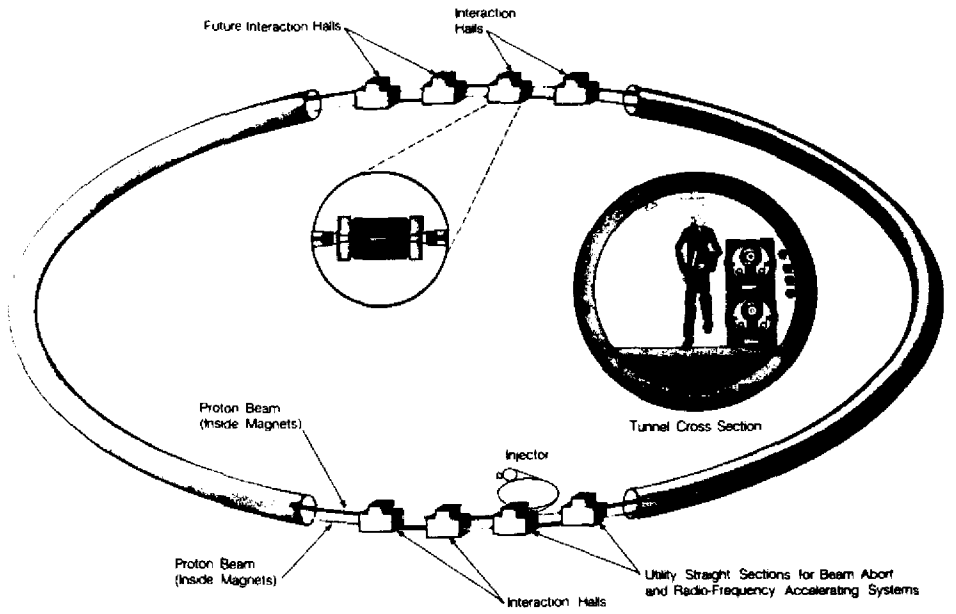

Figure 16: Collider ring layout envisaged in the SSC Conceptual Design Report.

The superconducting magnets essential for guiding the protons around the rings are made of two coils arranged to approximate a cosθ current distribution. The inner coil has an inside diameter of 4 cm. The coils are wound of cable made from composite strands containing thousands of filaments—each about 6μm in diameter—of a niobium-titanium alloy embedded in a copper matrix. Interlocking stainless steel or aluminum collars surrounded by an iron yoke hold the cables in place. This 17-meter-long package, called the "cold mass," is sealed in its own cryostat, where it can be maintained at an operating temperature of 4.35 K. The 3840 dipole magnets in each collider ring have a peak operating field of 6.6 teslas, which corresponds to a current of 6504 amperes. Figure 17 shows a cross section of the SSC dipole.

Substantial increases in the current-carrying capacity of superconducting cable have resulted from a collaboration among industry, university researchers, and the U.S. national laboratories focused on the development of improved superconductor for the SSC. The SSC specification for the critical current density in niobium-titanium strand, J_c = 2750 A/mm^2 at 4.2 K and 5 T, represents a 50 percent improvement over the conductor used in the Tevatron. Material meeting this demanding specification is now routinely received in production quantities.

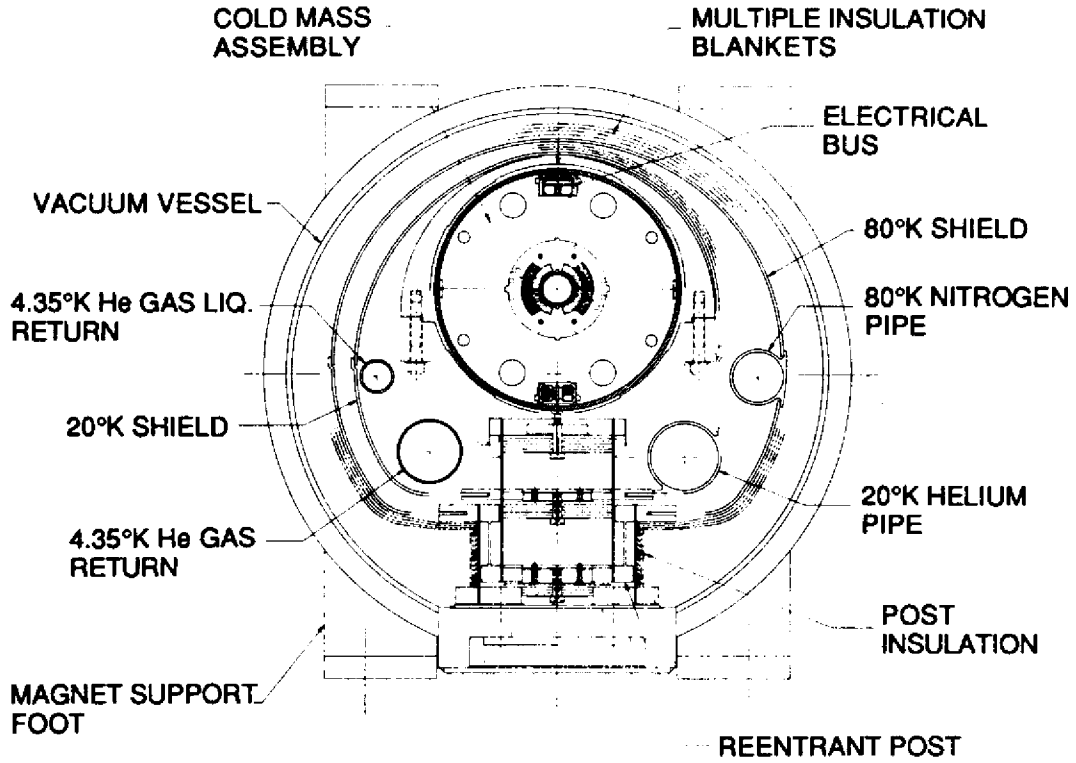

Figure 17: Cross section of the 6.6-tesla superconducting dipole magnet for the SSC.

When might the SSC be in operation? An important milestone was passed in March 1986, when the SSC Central Design Group completed a Conceptual Design Report for the SSC. Every major system had been thought through, and a detailed cost estimate had been made. Because a location had not been selected for the Supercollider, the Conceptual Design was not adapted for any specific site. During the summer of 1986, the Department of Energy and independent experts validated the cost and technical feasibility of the machine described in the Conceptual Design Report. President Reagan endorsed the SSC as a national goal in January 1987. In April of that year, the Department of Energy began a site search that has led to a short list of seven "Best Qualified Sites" in the states of Arizona, Colorado, Illinois, Michigan, North Carolina, Tennessee, and Texas. The Department of Energy intends to designate a preferred site in November 1988. From the time the site is available, sometime in 1989, it will take about

seven and a half years to build the machine. We hope to commence experimentation with the SSC by 1996.

We believe that the SSC can foster a new level of international cooperation in particle physics. As a frontier research instrument, the Supercollider will certainly attract to its experimental program many of the best particle physicists from around the world. This is of course traditional in our field, but we may hope for more: active international collaborations established early enough to allow significant foreign participation in the design and construction of the SSC and its detectors, and not just in the performance of experiments.

The advances of the past decade have brought us tantalizingly close to a profound new conception of the most basic constituents of matter and their interactions. The simpler and more comprehensive understanding we have gained organizes current knowledge and locates the horizon of particle physics at energies of trillions of electron volts, and the horizon of cosmology at about 10^{-15} second after the moment of creation. Important answers will be found with the Supercollider: from it we await new discoveries about the unification of the forces of nature and the patterns of the fundamental constituents of matter.

ACKNOWLEDGMENTS

It is a pleasure to thank Jack Schneps, Tom Kafka, and all of our hosts at Tufts for arranging a stimulating and enjoyable meeting with broad participation from around the globe.

FOOTNOTES AND REFERENCES

1. Proceedings of the 1988 HERA Workshop, edited by R. Peccei, DESY Report, 1988 (to be published).

2. T. Kirk, et al., Fermilab Proposal E-665.

3. R. Windmolders, Rapporteur's talk at the XXIV International Conference on High Energy Physics, Munich, August, 1988.

4. C. Quigg, M. H. Reno, and T. P. Walker, *Phys. Rev. Lett.* **57**, 774 (1986).

5. E. Eichten, I. Hinchliffe, K. D. Lane, and C. Quigg, *Rev. Mod. Phys.* **56**, 579 (1984); ibid. **58**, 1065E (1986).

6. Yu. M. Andreev, V. S. Berezinsky, and A. Yu. Smirnov, *Phys. Lett.* **84B**, 247 (1979).

7. D. MacKay and J. Ralston, *Phys. Lett.* **167B,** 103 (1986).

8. L. V. Gribov, E. M. Levin, and M. G. Ryskin, *Phys. Rep.* **100,** 1 (1983).

9. M. H. Reno and C. Quigg, *Phys. Rev. D*37, 657 (1988).

10. G. Danby, J.-M. Gaillard, K. Goulianos, L. M. Lederman, N. Mistry, M. Schwartz, and J. Steinberger, *Phys. Rev. Lett.* **9,** 36 (1962). For background information, see B. Pontecorvo, *ZhETF* **37,** 1751 (1959) [English translation: *Sov. Phys.—JETP* **37,** 1236 (1960)]; M. Schwartz, *Phys. Rev. Lett.* **4,** 306 (1960); T. D. Lee and C. N. Yang, ibid. **4,** 307 (1960).

11. C. Quigg, talk at the Fermilab Neutrino Bubble Chamber Workshop, Argonne National Laboratory, October 29, 1979; I. Pless, T. Kitagaki, et al., Fermilab Proposal E-636; C. Baltay, M. Peters, et al., Fermilab Proposal E-646; papers presented at the Fermilab Beam Dump Workshop, April 4, 1986.

12. C. Shipbaugh, et al., *Phys. Rev. Lett.* **60,** 2117 (1988).

13. W. J. Marciano, These Proceedings, p. .

14. For a summary of the standard shortcomings, see EHLQ, Ref. 5.

15. M. Veltman, *Acta. Phys. Pol. B* **12,** 437 (1981); C. H. Llewellyn Smith, *Phys. Rep.* **105,** 53 (1984).

16. Reviews of the experimental implications of supersymmetry on the scale of electroweak symmetry breaking appear in D. V. Nanopoulos and A. Savoy-Navarro (ed.), *Phys. Rep.* **105,** 1 (1984); H. E. Haber and G. L. Kane, ibid. **117,** 75 (1985); S. Dawson, E. Eichten, and C. Quigg, *Phys. Rev. D* **31,** 1581 (1985); R. M. Barnett, H. E. Haber, and G. L. Kane, *Nucl. Phys.* **B267,** 625 (1986).

17. For reviews of the technicolor idea, see E. Farhi and L. Susskind, *Phys. Rep.* **74,** 277 (1981); R. Kaul, *Rev. Mod. Phys.* **55,** 449 (1983). A study for the current generation of hadron colliders appears in E. Eichten, I. Hinchliffe, K. Lane, and C. Quigg, *Phys. Rev. D* **34,** 1547 (1986).

18. The idea of a strongly interacting gauge sector is an evergreen in particle theory. In the context of the standard model, early discussions appear in M. Veltman, *Acta. Phys. Pol. B* **8,** 475 (1977) and B. W. Lee, C. Quigg, and H. B. Thacker, *Phys. Rev. D* **16,** 1519 (1977). Recent investigations appropriate to the supercollider scale are reported in M. Chanowitz and M. K. Gaillard, *Nucl. Phys.* **B261,** 379 (1985); *Phys. Lett.* **142B,** 85 (1984); M. Chanowitz, M. Golden, and H. Georgi, *Phys. Rev. D* **36,** 1490 (1987).

19. M. Green and J. Schwarz, *Phys. Lett.* **149B,** 117 (1984); ibid. **151B,** 21 (1985); D. J. Gross, J. A. Harvey, E. Martinec, and R. Rolm, *Phys. Rev. Lett.* **54,**

502 (1985); *Nucl. Phys.* **B256,** 253 (1985); E. Witten, *Nucl. Phys.* **B258,** 75 (1985); M. Dine, V. Kaplunovsky, M. Mangano, C. Nappi, and N. Seiberg, *Nucl. Phys.* **B259,** 519 (1985).

20. L. S. Durkin and P. Langacker, *Phys. Lett.* **166B,** 436 (1986); P. Binétruy, S. Dawson, I. Hinchliffe, and M. Sher, *Nucl. Phys.* **B273,** 501 (1986); J. L. Rosner, in *Proceedings of the International Symposium on Particle and Nuclear Physics,* Beijing, 1985, edited by Ning Hu and Chong-Shi Wu (World Scientific, Singapore, 1986), p. 196; E. Cohen, J. Ellis, K. Enqvist, and D. V. Nanopoulos, *Phys. Lett.* **161B,** 85 (1985); ibid. **165,** 76 (1985); D. London and J. L. Rosner, *Phys. Rev. D* **34,** 1530 (1986); V. Barger, N. G. Deshpande, and K. Whisnant, *Phys. Rev. Lett.* **56,** 30 (1986); *Phys. Rev. D* **33,** 1912 (1986). Somewhat sharper bounds arise from a comparison of $\bar{x}_W \equiv 1 - M_W^2/M_Z^2$ with x_W measured in deeply inelastic neutrino scattering. See J. Ellis, K. Enqvist, D. V. Nanopoulos, and F. Zwirner, *Mod. Phys. Lett. A* **1,** 57 (1986); U. Amaldi, et al., *Phys. Rev. D* **36,** 1385 (1987).

21. B. L. Combridge, *Nucl. Phys.* **B151,** 429 (1979).

22. Z. Kunszt and E. Pietarinen, *Z. Phys. C* **2,** 335 (1979); Z. Kunszt, E. Pietarinen, and E. Reya, *Phys. Rev. D* **21,** 73 (1980); F. Halzen and P. Hoyer, *Phys. Lett.* **154B,** 324 (1985).

23. P. Nason, S. Dawson, and R. K. Ellis, *Nucl. Phys.* **B303,** 607 (1988).

24. W. Scott, in *Proceedings of the International Symposium on Physics of Proton-Antiproton Collision,* edited by Y. Shimizu and K. Takikawa (KEK, National Laboratory for High Energy Physics, Tsukuba, 1985), p. 68; G. Arnison, et al. (UA1 Collaboration), *Phys. Lett.* **177B,** 244 (1986).

25. G. Arnison, et al. (UA1 Collaboration), *Phys. Lett.* **172B,** 461 (1986).

26. The curves shown are 1.5 × the lowest-order QCD predictions, evaluated with $Q^2 = p_\perp^2$. The systematic errors on the data are ± 70%. Theoretical uncertainties are of a similar magnitude, but tend to increase the predicted cross section. See R. K. Ellis and J. C. Sexton, *Nucl. Phys.* **B269,** 445 (1986).

27. *Large Hadron Collider in the LEP Tunnel,* edited by G. Brianti, et al., CERN 84-10.

28. *Proceedings of the 1984 Summer Study on Design and Utilization of the Superconducting Super Collider,* edited by R. Donaldson and J. G. Morfín (Fermilab, Batavia, Illinois, 1984); *$\bar{p}p$ Options for the Supercollider,* edited by J. E. Pilcher and A. R. White (University of Chicago, 1984); *Physics at the*

Superconducting Super Collider Summary Report, edited by P. Hale and B. Winstein (Fermilab, 1984).

29. *Supercollider Physics,* edited by D. E. Soper (World Scientific, Singapore, 1986).

30. *Proceedings of the Summer Study on the Physics of the Superconducting Super Collider, Snowmass, 1986,* edited by R. Donaldson and J. Marx (Division of Particles and Fields of the American Physical Society, New York, 1987).

31. *Les Rencontres de Physique de la Vallée d'Aoste, Results and Perspectives in Particle Physics,* edited by M. Greco (Editions Frontières, Gif-sur-Yvette, France, 1987).

32. *Proceedings of the Workshop on Experiments, Detectors, and Experimental Areas for the Supercollider,* Berkeley, 1987, edited by R. Donaldson and M. G. D. Gilchriese (World Scientific, Singapore, 1988).

33. *Superconducting Super Collider Conceptual Design,* Central Design Group Report SSC-SR-2020 (March, 1986).

34. M. M. Block and R. N. Cahn, LBL-23472, to be published in the Proceedings of the Rockefeller University meeting on Elastic Scattering and Diffractive Processes, October, 1987.

35. A. Bassetto, M. Ciafaloni, G. Marchesini, *Phys. Rep.* **100,** 201 (1983).

36. A. H. Mueller, *Nucl. Phys.* **B213,** 85 (1983); ibid. **B228,** 351 (1983); ibid. **B241,** 141 (1984); J. B. Gaffney and A. H. Mueller, ibid. **B250,** 109 (1985). For a convenient review, see R. K. Ellis, in Ref. 29, p. 77.

37. A. H. Mueller and P. Nason, *Nucl. Phys.* **B266,** 265 (1986).

38. Preliminary results of the UA1 Collaboration for the fraction of gluon jets splitting into $c\bar{c}$ pairs are reported by M. Della Negra, in *6th Topical Workshop on Proton-Antiproton Collider Physics,* edited by K. Eggert, H. Faissner, and E. Radermacher (World Scientific, Singapore, 1987), p. 181.